Universal fractional map and cascade of bifurcations type attractors

M. Edelman

Citation: Chaos **23**, 033127 (2013); doi: 10.1063/1.4819165
View online: https://doi.org/10.1063/1.4819165
View Table of Contents: http://aip.scitation.org/toc/cha/23/3
Published by the American Institute of Physics

CHAOS **23**, 033127 (2013)

Universal fractional map and cascade of bifurcations type attractors

M. Edelman
Department of Physics, Stern College at Yeshiva University, 245 Lexington Ave, New York, New York 10016, USA and Courant Institute of Mathematical Sciences, New York University, 251 Mercer St., New York, New York 10012, USA

(Received 7 May 2013; accepted 11 August 2013; published online 26 August 2013)

We modified the way in which the Universal Map is obtained in the regular dynamics to derive the Universal α-Family of Maps depending on a single parameter $\alpha > 0$, which is the order of the fractional derivative in the nonlinear fractional differential equation describing a system experiencing periodic kicks. We consider two particular α-families corresponding to the Standard and Logistic Maps. For fractional $\alpha < 2$ in the area of parameter values of the transition through the period doubling cascade of bifurcations from regular to chaotic motion in regular dynamics corresponding fractional systems demonstrate a new type of attractors—cascade of bifurcations type trajectories. © *2013 AIP Publishing LLC*. [http://dx.doi.org/10.1063/1.4819165]

Fractional dynamical systems are systems that can be described by fractional differential equations (FDEs) with a fractional time derivative. FDEs are integro-differential equations and solutions of the nonlinear FDE require long runs of computations. This is why an investigation of the discrete maps which can be derived from the FDE, the fractional maps, is even more important for the study of the general properties of the nonlinear fractional dynamical systems than the investigation of the regular maps in the case of the regular nonlinear dynamical systems. In this article, we investigate the Universal α-Family of Maps (αFM) that depend on a single parameter—the order α ($\alpha > 0$) of the corresponding FDE with the periodic kicks. We show that the integer members of the family represent area/volume preserving maps and investigate their fixed/periodic points. Using the particular examples of the Logistic and Standard αFM, we show how the maps' properties evolve with the increase in α. The fractional dynamical systems are systems with memory and solutions of the FDE may possess quite unusual properties: trajectories may intersect, attractors may overlap, attractors exist in the asymptotic sense, and their limiting values may not belong to their basins of attraction. Cascade of bifurcations type trajectories (CBTTs) are a new type of attractors, which exists only in the fractional dynamical systems. In a CBTT, a cascade of bifurcations occurs not as a result of a change in a system's parameter (as in regular dynamical systems) but on a single attracting trajectory during its time evolution. We show that the CBTT exists in both families for $0 < \alpha < 1$. When $1 < \alpha < 2$, we found the areas of parameters in which the CBTT may exist in the Standard αFM and the inverse CBTT in the Logistic αFM. The particular areas of the application of the fractional maps may include biological systems (population biology, human memory, and adaptation) and fractional control.

I. INTRODUCTION

Fractional derivatives are integro-differential operators in which an integral is a convolution of a function (or its derivative) with a power function of a variable.[1–3] This is why FDEs are frequently used in science and engineering to describe systems with power law memory (see, e.g., Refs. 2–10). We will call systems which can be described by the FDE with a time fractional derivative fractional dynamical systems. Because FDEs are integro-differential equations and there are no high order numerical algorithms to simulate such equations, derivation of the fractional maps is important for the investigation of the general properties of the nonlinear fractional dynamical systems. The nonlinear fractional maps are also discrete convolutions. They model systems in which the present state depends on a function of all previous states weighted by a power of the time passed. Systems with power law memory include viscoelastic materials,[11] electromagnetic fields in dielectric media,[12–14] Hamiltonian systems,[4] etc.

There are many examples of systems with power law memory in biology. It has been shown recently[15,16] that processing of external stimuli by individual neurons can be described by fractional differentiation. There are multiple examples where power-law adaptation has been applied in describing the dynamics of biological systems at levels ranging from single ion channels up to human psychophysics.[17–22] Fluctuations within single protein molecules demonstrate power-law memory kernel with the exponent -0.51 ± 0.07.[23] The power law has been demonstrated in many cases in the research on human memory. Forgetting—the accuracy in a memory task at time t is given by $x = at^{-b}$, where $0 < b < 1$.[17,24–27] Learning also can be described by a power law. The reduction in reaction times that comes with practice is a power function of the number of training trials.[28]

In many cases,[3,29,30] FDEs are equivalent to the Volterra integral equations of the second kind. This kind of equation (not necessarily FDE) is used in nonlinear viscoelasticity (see, for example, Refs. 31 and 32) and in population biology and epidemiology, see Refs. 33 and 34. The very basic model in population biology is the ubiquitous Logistic Map. This map has been used to investigate the essential property of the nonlinear systems—transition from order to chaos through a sequence of period-doubling bifurcations, which is

called cascade of bifurcations, and its relation to the scaling properties of the corresponding systems (see Ref. 35). But the subjects of population biology are always systems with memory, which can be related to changes in DNA or, as in the case of human society, to legal regulations; and in most cases reproduction also involves time delay. Development and investigation of a map which would correspond to the Logistic Map with the power law memory and time delay is important not only for the population biology but also, as in the case of regular dynamics, it is important in order to study the general properties of the nonlinear fractional dynamical systems. One of the current main areas of the application of the nonlinear FDE, control theory (see Refs. 9 and 36), will also benefit from the study of the general properties of the fractional dynamical systems.

Nonlinear circuit elements with memory, memristors, memcapacitors, and meminductors[37,38] can be used to model nonlinear systems with memory. These elements may be common at the nanoscale, where the dynamical properties of charged particles depend on the history of a system.[38] Properties of such systems and their fractional generalizations[39,40] are already a subject of research but at present mathematical modeling of the fractional maps remains the most useful for the study of the general properties of the fractional dynamical systems.

The first fractional maps were derived from the FDE in Refs. 30 and 41–43. The first results of the investigation of the fractional maps (see Refs. 42–45) revealed new properties of the fractional dynamical systems: intersection of trajectories, overlapping of chaotic attractors, and existence of the attractors in the asymptotic sense (the limiting values may not belong to their basins of attraction). CBTTs are the most unusual features of the investigated fractional maps. In the CBTT, a cascade of bifurcations is not a result of the change in a system parameter (as in the regular dynamics) but appears as the attracting single trajectory and is a new type of attractors. All previous investigations of the fractional maps were done on the various forms of the fractional two-dimensional Standard Map corresponding to the order $1 < \alpha \leq 2$ of the fractional derivative. The CBTT appeared in all investigated fractional maps. The consideration of the origin and the necessary and sufficient conditions of the CBTT's existence requires further investigation of the fractional maps, which includes development of the simple, if possible one-dimensional, fractional maps. The Logistic Map, and the maps with $\alpha \leq 1$ in general, cannot be derived in a way previously used in Refs. 7 and 30 to derive the fractional maps for $\alpha > 1$ (for a detailed discussion see Ref. 46). In Ref. 46, we introduced the notions of the Universal Fractional Map of an arbitrary order $\alpha > 0$ and the αFM, which allow a uniform derivation of the fractional maps of the order $\alpha > 0$. In this paper, we continue the investigation of the Universal Fractional Map (Sec. II) and investigate the general properties (fixed and periodic points and their stability) for the Universal Fractional Map of an arbitrary integer order (Sec. II B). We also conduct the detailed investigation of the members of the Logistic αFM with $\alpha \leq 2$ (Secs. III and IV). As it has been shown before for the members of the Standard αFM with $\alpha \leq 2$, in the Logistic αFM the CBTT exists for the fractional values of α but when $1 < \alpha < 2$ the Logistic αFM demonstrate only the inverse CBTT (Sec. IV C).

II. UNIVERSAL FRACTIONAL MAP

To derive the equations of the Universal αFM, let us start with the equation introduced in Ref. 46

$$\frac{d^\alpha x}{dt^\alpha} + G_K(x(t-\Delta T)) \sum_{k=-\infty}^{\infty} \delta\left(\frac{t}{T} - (k+\varepsilon)\right) = 0, \quad (1)$$

where $\varepsilon > \Delta > 0$, $\alpha \in \mathbb{R}$, $\alpha > 0$, in the limit $\varepsilon \to 0$. The initial conditions should correspond to the type of fractional derivative we are going to use. In the case $\alpha = 2$, $\Delta = 0$, and $G_K(x) = KG(x)$, Eq. (1) corresponds to the equation whose integration produces the regular Universal Map (see Ref. 4). Case $\Delta = 0$ and $G_K(x) = KG(x)$ has been used to derive the fractional Universal Map for $\alpha > 1$ (see Chap. 18 from Ref. 7). $\Delta \neq 0$ is essential for the case $\alpha \leq 1$ when $x(t)$ is a function discontinued at the time of the kicks[41,46] and the use of the K as a parameter rather than a factor is necessary to extend the class of the considered maps to include the Logistic Map (see Sec. III). Without losing the generality, we assume $T = 1$. Case $T \neq 1$ is considered in Ref. 46 and can be reduced to this case by rescaling the time variable. Further, in the paper T denotes periods of trajectories.

A. Riemann-Liouville universal fractional map

In the case of the Riemann-Liouville fractional derivative, Eq. (1) can be written as

$${}_0D_t^\alpha x(t) + G_K(x(t-\Delta)) \sum_{k=-\infty}^{\infty} \delta(t-(k+\varepsilon)) = 0, \quad (2)$$

where $\varepsilon > \Delta > 0$, $\varepsilon \to 0$, $0 \leq N-1 < \alpha \leq N, \alpha \in \mathbb{R}, N \in \mathbb{N}$, and the initial conditions

$$({}_0D_t^{\alpha-k} x)(0+) = c_k, \quad (3)$$

where $k = 1,\ldots, N$. The left-sided Riemann-Liouville fractional derivative ${}_0D_t^\alpha x(t)$ defined for $t > 0$ (Refs. 1–3) as

$$\begin{aligned} {}_0D_t^\alpha x(t) &= D_t^n \, {}_0I_t^{n-\alpha} x(t) \\ &= \frac{1}{\Gamma(n-\alpha)} \frac{d^n}{dt^n} \int_0^t \frac{x(\tau)d\tau}{(t-\tau)^{\alpha-n+1}}, \end{aligned} \quad (4)$$

where $n-1 \leq \alpha < n$, $n \in \mathbb{Z}$, $D_t^n = d^n/dt^n$, ${}_0I_t^\alpha$ is a fractional integral, and $\Gamma()$ is the gamma function.

This problem (Eqs. (2) and (3)) can be reduced[3,7,29] to the Volterra integral equation of the second kind for $t > 0$

$$\begin{aligned} x(t) &= \sum_{k=1}^{N} \frac{c_k}{\Gamma(\alpha-k+1)} t^{\alpha-k} \\ &\quad - \frac{1}{\Gamma(\alpha)} \int_0^t d\tau \frac{G_K(x(\tau-\Delta))}{(t-\tau)^{1-\alpha}} \sum_{k=-\infty}^{\infty} \delta(\tau-(k+\varepsilon)), \end{aligned} \quad (5)$$

which integration gives ($t > 0$)

$$x(t) = \sum_{k=1}^{N-1} \frac{c_k}{\Gamma(\alpha-k+1)} t^{\alpha-k} - \frac{1}{\Gamma(\alpha)} \sum_{k=0}^{[t-\varepsilon]} \frac{G_K(x(k+\varepsilon-\Delta))}{(t-(k+\varepsilon))^{1-\alpha}} \Theta(t-(k+\varepsilon)), \quad (6)$$

where $\Theta(t)$ is the Heaviside step function. In Eq. (6), we took into account that boundedness of $x(t)$ at $t=0$ requires $c_N = 0$ and $x(0)=0$ (see Refs. 1–3 and 47).

With the introduction[41] $p(t) = {}_0D_t^{\alpha-N+1}x(t)$, $p^{(s)}(t) = D_t^s p(t)$, $s=0, 1,\ldots, N-2$ Eq. (6) leads to

$$p^{(s)}(t) = \sum_{k=1}^{N-s-1} \frac{c_k}{(N-s-1-k)!} t^{N-s-1-k} - \frac{1}{(N-s-2)!} \sum_{k=0}^{[t-\varepsilon]} G_K(x(k+\varepsilon-\Delta))(t-k)^{N-s-2}, \quad (7)$$

where $s=0, 1,\ldots, N-2$. With the definitions $x_n = x(n)$ and $p_n^{(s)} = p^{(s)}(n)$, Eqs. (6) and (7) in the limit $\varepsilon \to 0$ give for t = n + 1 the Riemann-Liouville Universal αFM

$$x_{n+1} = \sum_{k=1}^{N-1} \frac{c_k}{\Gamma(\alpha-k+1)} (n+1)^{\alpha-k} - \frac{1}{\Gamma(\alpha)} \sum_{k=0}^{n} G_K(x_k)(n-k+1)^{\alpha-1}, \quad (8)$$

$$p_{n+1}^s = \sum_{k=1}^{N-s-1} \frac{c_k}{(N-s-1-k)!} (n+1)^{N-s-1-k} - \frac{1}{(N-s-2)!} \sum_{k=0}^{n} G_K(x_k)(n-k+1)^{N-s-2}. \quad (9)$$

The map equations for momentum are defined in a usual way

$$p(t) = D_t^1 x(t), \quad p^s(t) = D_t^s p(t), \quad s = 0, 1, \ldots, N-2, \quad (10)$$

and the discussion on the different ways of the defining momentum in the case of the Riemann-Liouville maps can be found in Ref. 46. Riemann-Liouville Universal αFM equations (8) and (9) can be written in the much simpler form

$$p_{n+1}^s = p_n^s + \sum_{k=0}^{N-s-3} \frac{p_n^{k+s+1}}{(k+1)!} - \frac{G_K(x_n)}{(N-s-2)!}, \quad (11)$$

$$x_{n+1} = \sum_{k=2}^{N-1} \frac{c_k}{\Gamma(\alpha-k+1)} (n+1)^{\alpha-k} + \frac{1}{\Gamma(\alpha)} p_{n+1}^{N-2} + \frac{1}{\Gamma(\alpha)} \sum_{k=0}^{n-1} p_{k+1}^{N-2} V_\alpha^1(n-k+1), \quad (12)$$

where $s=0, 1,\ldots N-2$ and $V_\alpha^k(m) = m^{\alpha-k} - (m-1)^{\alpha-k}$.

B. Integer-dimensional universal maps

For the integer $\alpha = N$, the Universal αFM converges to

$$p_{n+1}^s = p_n^s + \sum_{k=0}^{N-s-3} \frac{p_n^{k+s+1}}{(k+1)!} - \frac{G_K(x_n)}{(N-s-2)!}, \quad (13)$$

$$x_{n+1} = x_n + \sum_{k=0}^{N-2} \frac{p_n^k}{(k+1)!} - \frac{G_K(x_n)}{(N-1)!}. \quad (14)$$

To prove that for $N \geq 2$, the map equations (13) and (14) are the N-dimensional volume preserving map, let us consider the determinant of its Jacobian $N \times N$ matrix $J(x_0, p_0^0, \ldots, p_0^{N-2})$

$$\begin{vmatrix} 1-\frac{\dot{G}_K(x)}{\Gamma(N)} & 1 & \frac{1}{2} & \ldots & \frac{1}{\Gamma(n)} & \ldots & \frac{1}{\Gamma(N-1)} & \frac{1}{\Gamma(N)} \\ -\frac{\dot{G}_K(x)}{\Gamma(N-1)} & 1 & 1 & \ldots & \frac{1}{\Gamma(n-1)} & \ldots & \frac{1}{\Gamma(N-2)} & \frac{1}{\Gamma(N-1)} \\ -\frac{\dot{G}_K(x)}{\Gamma(N-2)} & 0 & 1 & \ldots & \frac{1}{\Gamma(n-2)} & \ldots & \frac{1}{\Gamma(N-3)} & \frac{1}{\Gamma(N-2)} \\ \ldots & \ldots & \ldots & \ldots & \ldots & \ldots & \ldots & \ldots \\ -\frac{\dot{G}_K(x)}{\Gamma(N-k+1)} & 0 & 0 & \ldots & \frac{1}{\Gamma(n-k+1)} & \ldots & \frac{1}{\Gamma(N-k)} & \frac{1}{\Gamma(N-k+1)} \\ \ldots & \ldots & \ldots & \ldots & \ldots & \ldots & \ldots & \ldots \\ -\dot{G}_K(x) & 0 & 0 & \ldots & 0 & \ldots & 0 & 1 \end{vmatrix},$$

where n and k are the column and row numbers. The first column can be written as the sum of the column with one in the first row and the remaining zeros and the column, which is equal to $\dot{G}_K(x)$ times the last column. Determinants of the corresponding matrices are 1 and 0; this is why the Jacobian determinant is equal to one and the map is the N-dimensional volume preserving map.

The integer Universal αFM's fixed points are $p_0^s = 0$ $(s = 0, \ldots, N-2)$ and x_0 satisfies $G(x_0) = 0$. Their stability for $N \geq 1$ is defined by the eigenvalues λ of the Jacobian

matrix. Polynomial $P(\lambda) = \det[J(x_0, p_0^0, \ldots, p_0^{N-2}) - \lambda I]$ has values $P(0) = \lambda_1 \times \ldots \times \lambda_N = 1$ and $P(1) = (-1)^N \dot{G}_K(x_0)$, which means that for odd values of $N > 1$ stability is possible only if $\dot{G}_K(x_0) = 0$. For period two ($T = 2$) points $p_{n+1}^s = -p_n^s$ ($s = 0, \ldots, N-2$) and $G(x_{n+1}) = -G(x_n)$. In the case $N = 3$, the only $T = 2$ points are the fixed points.

C. Caputo universal fractional map

For Eq. (1) with the left-sided Caputo derivative,[3]

$$\begin{aligned} {}_0^C D_t^\alpha x(t) &= {}_0 I_t^{n-\alpha} D_t^n x(t) \\ &= \frac{1}{\Gamma(n-\alpha)} \int_0^t \frac{D_\tau^n x(\tau) d\tau}{(t-\tau)^{\alpha-n+1}} \quad (n-1 < \alpha \le n), \end{aligned} \tag{15}$$

the initial conditions may be taken as $(D_t^k x)(0+) = b_k$, $k = 0, \ldots, N-1$. This problem is equivalent to the Volterra integral equation of the second kind ($t > 0$)

$$\begin{aligned} x(t) = &\sum_{k=0}^{N-1} \frac{b_k}{k!} t^k \\ &- \frac{1}{\Gamma(\alpha)} \int_0^t d\tau \frac{G_K(x(\tau - \Delta))}{(t-\tau)^{1-\alpha}} \sum_{k=-\infty}^{\infty} \delta(\tau - (k + \varepsilon)). \end{aligned} \tag{16}$$

With the introduction $x^{(s)}(t) = D_t^s x(t)$, the Caputo Universal αFM can be derived in the form[7]

$$\begin{aligned} x_{n+1}^{(s)} = &\sum_{k=0}^{N-s-1} \frac{x_0^{(k+s)}}{k!} (n+1)^k \\ &- \frac{1}{\Gamma(\alpha - s)} \sum_{k=0}^{n} G_K(x_k)(n-k+1)^{\alpha-s-1}, \end{aligned} \tag{17}$$

where $s = 0, 1, \ldots, N-1$.

III. INTEGER-DIMENSIONAL STANDARD AND LOGISTIC MAPS

Fractional map equations (11), (12), and (17) are maps with memory in which the next value of the map variables depends on all previous values. An increase in α leads to the increase in the dimension of the map and to the increased power in the power law dependence of the weights of the old states (the increased role of memory). Integer values of α correspond to the degenerate cases in which map equations can be written as the maps with full memory,[48] which are equivalent to the one step memory maps in which map variables at each step accumulate information about all previous states of the corresponding systems (for a discussion on the fractional maps as maps with memory see Ref. 46). To fully understand the properties of fractional maps, we will start with the consideration of the integer members of the corresponding families of maps.

In the $\alpha = 2$ case, Eqs. (13) and (14) produce the Standard Map if $G_K(x) = K \sin(x)$ and in the $\alpha = 1$ case, the Logistic Map results from $G_K(x) = x - Kx(1-x)$. We will call the Universal αFM Eqs. (11) and (12) with $G_K(x) = K \sin(x)$ the Standard Riemann-Liouville αFM and with $G_K(x) = x - Kx(1-x)$ the Logistic Riemann-Liouville αFM; we will call Universal αFM Eq. (17) with $G_K(x) = K \sin(x)$ the Standard Caputo αFM and with $G_K(x) = x - Kx(1-x)$ the Logistic Caputo αFM.

For $\alpha = 0$, the solution of Eq. (1) is identical zero. For $\alpha < 1$, the Universal Riemann-Liouville αFM Eq. (8) also produces identical zero for maps that satisfy $G(0) = 0$, which is true for the Standard Riemann-Liouville αFM and Logistic Riemann-Liouville αFM.

There are no stable fixed points in the $\alpha = 3$ Standard Map. For $K^2 - 16 < 4p^{12} < K^2$, there exist two lines of the stable $T = 2$ on the torus ballistic points. For more on the preliminary results of the investigation of the Standard αFM and Logistic αFM for $2 < \alpha \le 3$, see Ref. 46. A different form of the 3D Standard Map has been recently introduced and investigated in Ref. 49 and some 3D quadratic volume preserving maps were investigated in Ref. 50. The Standard αFM and Logistic αFM with $\alpha > 2$ are poorly investigated and 3D volume preserving maps, in general, are not fully investigated. In our simulations of the fractional maps, we were able to find the CBTT only for $\alpha < 2$. This is why in the present article we will not further consider maps with $\alpha > 2$.

A. One-dimensional maps

The $\alpha = 1$ Standard Riemann-Liouville αFM is a particular form of the Circle Map with zero driving phase

$$x_{n+1} = x_n - K \sin(x_n), \quad (\mathrm{mod}\, 2\pi). \tag{18}$$

The bifurcation diagrams for the regular Logistic Map and the one-dimensional Standard Map are presented in Fig. 1.

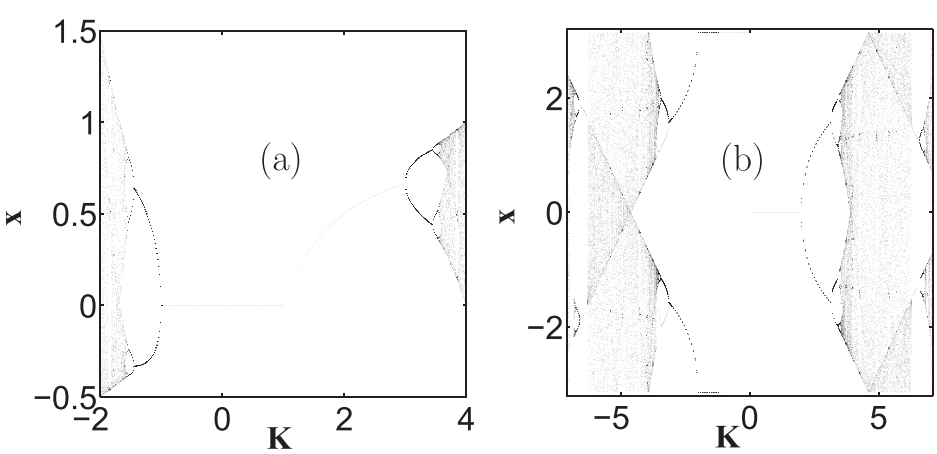

FIG. 1. (a) The bifurcation diagram for the regular Logistic Map $x = Kx(1-x)$. (b) The bifurcation diagram for 1D Standard Map, Eq. (18).

The 1D Standard Map has the attracting fixed points $2\pi n$ for $0 < K < 2$ and $\pi + 2\pi n$ when $-2 < K < 0$ (see Fig. 1(b)). The antisymmetric $T = 2$ points are stable for $2 < |K| < \pi$, while $x_{n+1} = x_n + \pi$ sinks ($T = 2$) are stable when $\pi < |K| < \sqrt{\pi^2 + 2} \approx 3.445$. The stable $T = 4$ sink appears at $K \approx 3.445$ and the transition to chaos through the period doubling cascade of bifurcations occurs at $K \approx 3.532$. More on the properties of the $\alpha = 1$ Standard Map can be found in Ref. 46.

Stability properties of the Logistic Map are well known.[51] For $K > 0$, the $x = 0$ fixed point is stable when $K < 1$, the $(K - 1)/K$ fixed point is stable when $1 < K < 3$, the $T = 2$ sink is stable for $3 \le K < 1 - \sqrt{6} \approx 3.449$, the $T = 4$ sink is stable for $3.449 < K < 3.544$, and at $K \approx 3.56995$ is the onset of chaos, at the end of the period-doubling cascade of bifurcations.

B. Two-dimensional maps

The regular ($\alpha = 2$) Standard Map (Chirikov Standard Map)

$$\begin{aligned} p_{n+1} &= p_n - K \sin x, \quad (\mathrm{mod}\, 2\pi), \\ x_{n+1} &= x_n + p_{n+1}, \quad (\mathrm{mod}\, 2\pi) \end{aligned} \tag{19}$$

demonstrates a universal generic behavior of the area-preserving maps whose phase space is divided into elliptic islands of stability and areas of chaotic motion and is well investigated (see, e.g., Ref. 52). In the Standard αFM with $1 < \alpha < 2$, the elliptic islands evolve into periodic sinks.[42,44–46] The properties of the phase space and the appearance of the CBTT in the Standard αFM are connected to the evolution (with the increase in parameter K) of the regular Standard Map's islands originating from the stable for $K < 4$ fixed point (0,0). At $K = 4$, it becomes unstable (elliptic-hyperbolic point transition) and two elliptic islands around the stable for $4 < K < 2\pi$ period 2 antisymmetric ($p_{n+1} = -p_n$, $x_{n+1} = -x_n$) points appear. At $K = 2\pi$, this point turns into the $T = 2$ point with $p_{n+1} = -p_n$, $x_{n+1} = x_n - \pi$, which is stable for $2\pi < K < 6.59$. The $T = 4$ stable elliptic points appear at $K \approx 6.59$ and the period doubling cascade of bifurcations leads to the disappearance of the islands of stability in the chaotic sea at $K \approx 6.6344$.[52]

The $\alpha = 2$ Logistic Map

$$\begin{aligned} p_{n+1} &= p_n + K x_n (1 - x_n) - x_n, \\ x_{n+1} &= x_n + p_{n+1} \end{aligned} \tag{20}$$

is a quadratic area preserving map. The quadratic area preserving maps with a stable fixed point at the origin were studied by Hénon[53] and a recent review on quadratic maps can be found in Ref. 54. The map equation (20) has two fixed points: (0, 0) stable for $K \in (-3, 1)$ and $((K - 1)/K, 0)$ stable for $K \in (1, 5)$. The $T = 2$ elliptic point

$$\begin{aligned} x &= \frac{K + 3 \pm \sqrt{(K+3)(K-5)}}{2K}, \\ p &= \pm \frac{\sqrt{(K+3)(K-5)}}{K} \end{aligned} \tag{21}$$

is stable for $-2\sqrt{5} + 1 < K < -3$ and $5 < K < 2\sqrt{5} + 1$. The period doubling cascade of bifurcations (for $K > 0$) with further bifurcations, $T = 2 \to T = 4$ at $K \approx 5.472$, $T = 4 \to T = 8$ at $K \approx 5.527$, $T = 8 \to T = 16$ at $K \approx 5.5319$, $T = 16 \to T = 32$ at $K \approx 5.53253$, etc., and the corresponding decrease in the area of the islands of stability leads to chaos (see Fig. 2).

IV. THE FRACTIONAL ($\alpha < 2$) STANDARD αFM AND LOGISTIC αFM

A. The CBTT in the standard αFM and the logistic αFM with $\alpha < 1$

With the corresponding $G_K(x)$, the Universal Caputo αFM for $0 < \alpha < 1$

$$x_{n+1} = x_0 - \frac{1}{\Gamma(\alpha)} \sum_{k=0}^{n} G(x_k)(n - k + 1)^{\alpha - 1} \tag{22}$$

produces the Standard Caputo αFM

$$x_n = x_0 - \frac{K}{\Gamma(\alpha)} \sum_{k=0}^{n-1} \frac{\sin x_k}{(n-k)^{1-\alpha}}, \ (\mathrm{mod}\, 2\pi), \tag{23}$$

and the Logistic Caputo αFM

$$x_n = x_0 + \frac{1}{\Gamma(\alpha)} \sum_{k=0}^{n-1} \frac{K x_k (1 - x_k) - x_k}{(n-k)^{1-\alpha}}, \tag{24}$$

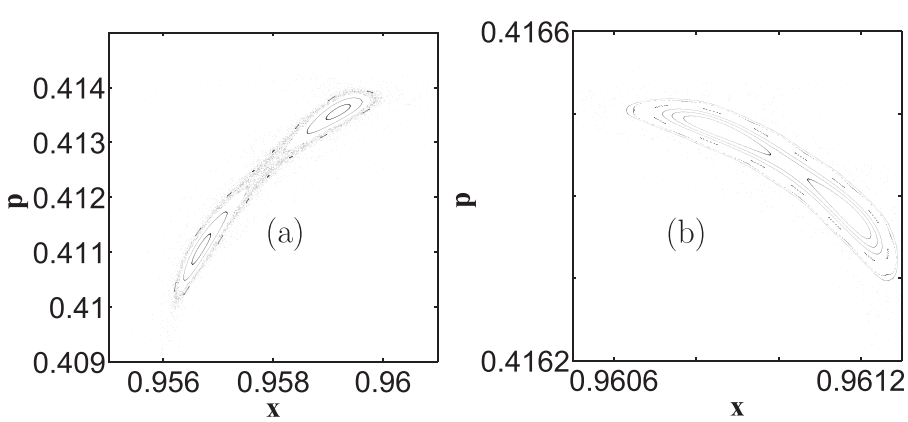

FIG. 2. Bifurcations in the 2D Logistic Map: (a) $T = 4 \to T = 8$ bifurcation at $K \approx 5.527$. (b) $T = 8 \to T = 16$ bifurcation at $K \approx 5.5319$.

which are one dimensional maps with the power law decreasing memory.[46] The bifurcation diagrams for these maps are similar to the corresponding diagrams for the $\alpha = 1$ case but are stretched along the parameter K-axis and the stretchiness increases with the decrease in α, Figs. 3(a)–3(d). In the area of the parameter values for which on the bifurcation diagram stable periodic $T > 2$ points exist, individual trajectories are the CBTT Figs. 3(e) and 3(f).

B. The CBTT in the standard αFM with 1 < α < 2

The Standard Riemann-Liouville and Caputo αFM with $1 < \alpha < 2$ were investigated in Refs. 42, 44, and 45. In this subsection, we will recall some of the results of this investigation. The fixed point (0, 0), which is a sink in this case, is stable for (see Fig. 4(a))

$$0 < K < K_{c1}(\alpha) = \frac{2\Gamma(\alpha)}{V_{\alpha l}}, \tag{25}$$

where

$$V_{\alpha l} = \sum_{k=1}^{\infty} (-1)^{k+1} V_{\alpha}^{1}(k). \tag{26}$$

In accordance with Sec. III, $K_{c1}(1) = 2$ and $K_{c1}(2) = 4$. The antisymmetric period 2 sink

$$p_{n+1} = -p_n, \; x_{n+1} = -x_n \tag{27}$$

is stable for $K_{c1}(\alpha) < K < K_{c2}(\alpha)$, where $K_{c2}(\alpha) = 0.5\pi K_{c1}(\alpha)$ with $K_{c2}(1) = \pi$ and $K_{c2}(2) = 2\pi$.

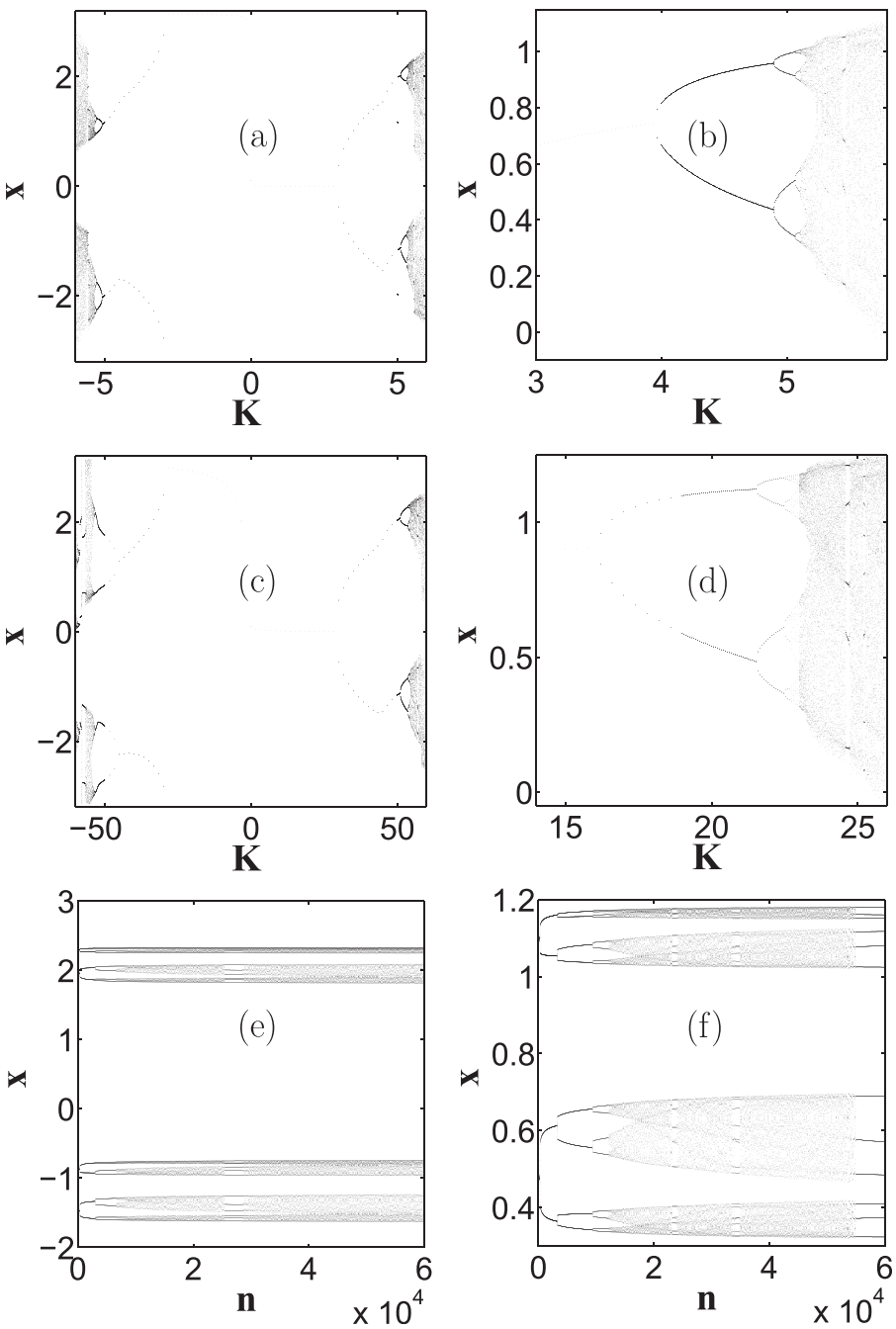

FIG. 3. Bifurcations and the CBTT in the Standard (Figures 3(a), 3(c), and 3(e)) and Logistic (Figures 3(b), 3(d), and 3(f)) Caputo αFM with $0 < \alpha < 1$. In (a)–(d), bifurcation diagrams obtained after performing 10^4 iterations on a single trajectory with $x_0 = 0.1$ for various values of K. In (a) and (b), $\alpha = 0.5$. In (c), $\alpha = 0.05$. In (d), $\alpha = 0.1$. In (e), a CBTT for $\alpha = 0.01$ and $K = 276$. In (f), a CBTT for $\alpha = 0.1$ and $K = 22.7$.

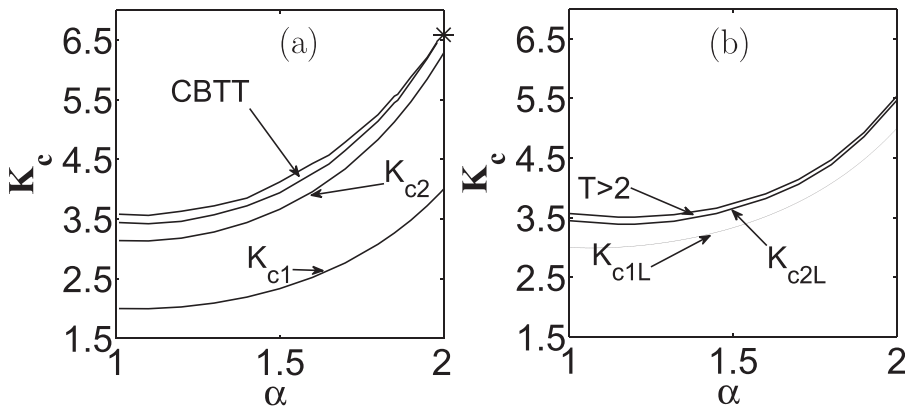

FIG. 4. Bifurcations in the Standard and Logistic αFM with $1 < \alpha < 2$. (a) The Standard αFM $K - \alpha$ graph. The fixed point (0, 0) is stable for $K < K_{c1}$; the anti-symmetric $T = 2$ sink is stable for $K_{c1} < K < K_{c2}$; two $T = 2$ sinks $x_{n+1} = x_n - \pi$, $p_{n+1} = -p_n$ are stable in a band above K_{c2}; the CBTT exists in the band of the map's parameters ending at the cusp in the top right corner; the upper curve is a border with chaos. The star marks the point ($K \approx 6.63$) at which the Standard Map's ($\alpha = 2$) $T = 2$ points become unstable and the $T = 4$ elliptic points are born. (b) The Logistic αFM $K - \alpha$ graph. One fixed point is stable for $K < K_{c1L}$; the $T = 2$ sink is stable for $K_{c1L} < K < K_{c2L}$; the sinks with $T \geq 4$ and the inverse CBTT exists in the upper band; the upper curve is a border with chaos.

$$p_{n+1} = -p_n, \; x_{n+1} = x_n + \pi \tag{28}$$

two T = 2 sinks are stable in the band above $K = K_{c2}(\alpha)$ curve (Fig. 4(a)). For $\alpha = 1$, it corresponds to $\pi < |K| < \sqrt{\pi^2 + 2} \approx 3.445$ and for the regular Standard Map the corresponding elliptic points are stable when $2\pi < K < 6.59$.

For $\alpha = 1$, the $T = 4$ sink appears at $K \approx 3.445$ and the transition to chaos occurs at $K \approx 3.532$ (Sec. III A), while for $\alpha = 2$ the $T = 4$ elliptic points appear at $K \approx 6.59$ and the sequence of the period doubling bifurcations leads to the disappearance of the islands of stability in chaotic sea at $K \approx 6.6344$ (Sec. III B). For $1 < \alpha < 2$, the CBTT exists in the band between two curves connecting the above-mentioned points (Fig. 4(a)). Both curves are calculated numerically and confirmed by the large number of computer simulations.[44,45] Within the CBTT, band trajectories evolve from being very stable features, which exist for the longest time we were running our codes, 500 000 iterations, when α is close to 1 (Fig. 5(a)) to being barely distinguishable and short-lived features when α is close to 2 (Fig. 5(b)). For the intermediate values of α, CBTT behaves similar to the sticky trajectories in Hamiltonian dynamics: occasionally

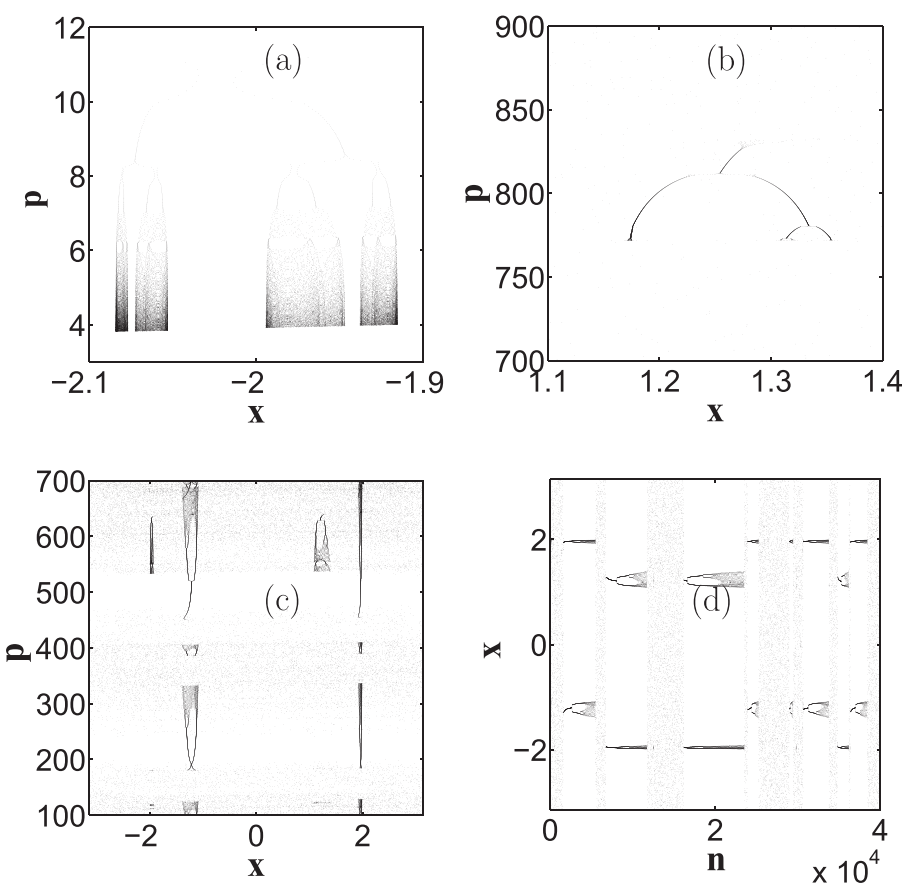

FIG. 5. A single CBTT in the Standard Riemann-Liouville αFM. (a) One of the two branches of the CBTT for $\alpha = 1.1$ and $K = 3.5$. (b) A zoom of a small feature in an intermittent trajectory for $\alpha = 1.95$ and $K = 6.2$. (c) An intermittent trajectory in phase space for $\alpha = 1.65$ and $K = 4.5$. (d) x of n for the case (c).

trajectories enter CBTT and then leave them entering the chaotic sea (Figs. 5(c) and 5(d)).

Let us list below some additional interesting properties of the Standard αFM with $1 < \alpha < 2$.[44,45] The types of solutions include periodic sinks, attracting slow diverging trajectories, attracting accelerator mode trajectories, chaotic attractors, and the CBTT. All attractors below the CBTT band are periodic sinks and slow diverging trajectories and all trajectories converge to one of those attractors. Each attractor has its own basin of attraction and the chaotic areas exist in the sense that two trajectories with infinitely close initial conditions from those areas may converge to different attractors. Periodic sinks exist in the limiting sense and the limiting values themselves in most of the cases do not belong to their basins of attraction. The rate of convergence of trajectories to the sinks depends on the initial conditions. The trajectories that start from the basins of attraction converge fast as $\delta x \sim n^{-1-\alpha}$, $\delta p \sim n^{-\alpha}$, while those starting from the chaotic areas converge slow as $\delta x \sim n^{-\alpha}$ (or even as $\delta x \sim n^{1-\alpha}$), $\delta p \sim n^{1-\alpha}$. Trajectories may intersect and chaotic attractors overlap. More on the properties of the Standard Riemann-Liouville and Caputo αFM with $1 \le \alpha \le 2$ can be found in Refs. 44–46.

C. CBTT in the logistic αFM with 1 < α < 2

In this part, we will investigate the Logistic Riemann-Liouville αFM

$$p_{n+1} = p_n + Kx_n(1 - x_n) - x_n, \tag{29}$$

$$x_{n+1} = \frac{1}{\Gamma(\alpha)} \sum_{i=0}^{n} p_{i+1} V_\alpha^1(n - i + 1). \tag{30}$$

As in the case of the Standard αFM, the partition of the phase space into the areas of stability of the periodic sinks originating from the period one sink (0, 0) is almost the same (numerical result) for the Logistic Riemann-Liouville and Caputo αFM. For $0 < K < 1$, all converging trajectories converge to (0, 0) point as $x \sim n^{-\alpha-1}$, $p \sim n^{-\alpha}$. For $1 < K < K_{c1L}$, the only stable sink is the period one $((K-1)/K, 0)$ sink and the rate of convergence is $\delta x \sim n^{-\alpha}$, $p \sim n^{-\alpha+1}$. For $K_{c1L} < K < K_{c2L}$, all converging trajectories (this is a result from the large number of numerical simulations) converge to the $T = 2$ sink antisymmetric in p (Fig. 6(a)).

To find the Logistic Riemann-Liouville αFM's critical curve K_{c1L} on which, as a result of a bifurcation, the $T = 1$ sink disappears and the $T = 2$ sink is born, let us consider the $T = 2$ sinks. The results of large number of simulations (see, e.g., Fig. 6(b)) suggest the following asymptotic behavior:

$$p_n = p_l(-1)^n + \frac{A}{n^{\alpha-1}} \ . \tag{31}$$

Then, from Eq. (30)

$$\begin{aligned} x_{lo} = \lim_{n\to\infty} x_{2n+1} &= \frac{p_l}{\Gamma(\alpha)} \lim_{n\to\infty} \sum_{k=1}^{2n+1} (-1)^k V_\alpha^1(k) \\ &+ \frac{A}{\Gamma(\alpha)} \lim_{n\to\infty} \sum_{k=1}^{2n-1} \frac{\alpha - 1}{k^{\alpha-1}(2n-k)^{2-\alpha}} = -\frac{p_l}{\Gamma(\alpha)} V_{\alpha l} \\ &+ \frac{(\alpha-1)A}{\Gamma(\alpha)} \int_0^1 \frac{x^{1-\alpha}dx}{(1-x)^{2-\alpha}} = -\frac{p_l}{\Gamma(\alpha)} V_{\alpha l} + A\Gamma(2-\alpha). \end{aligned} \tag{32}$$

In a similar way,

$$x_{le} = \lim_{n\to\infty} x_{2n} = \frac{p_l}{\Gamma(\alpha)} V_{\alpha l} + A\Gamma(2-\alpha). \tag{33}$$

In the limit $n \to \infty$, Eq. (29) gives

$$-2p_l = Kx_{le}(1 - x_{le}) - x_{le}, \tag{34}$$

$$2p_l = Kx_{lo}(1 - x_{lo}) - x_{lo}. \tag{35}$$

The system of Eqs. (32)–(35) has four equations and four unknown variables p_l, A, x_{lo}, and x_{le}. This equation has two obvious solutions $x_{lo} = x_{le} = p_l = A = 0$ and $x_{lo} = x_{le} = x_l = (K-1)/K$, $p_l = 0$, $A = x_l/\Gamma(2-\alpha)$, corresponding to two fixed points. If $x_{lo} \neq x_{le}$, then

$$A = \frac{K - 1 + \frac{2\Gamma(\alpha)}{V_{\alpha l}}}{2K\Gamma(2-\alpha)} \tag{36}$$

and x_{le} is a solution of the quadratic equation

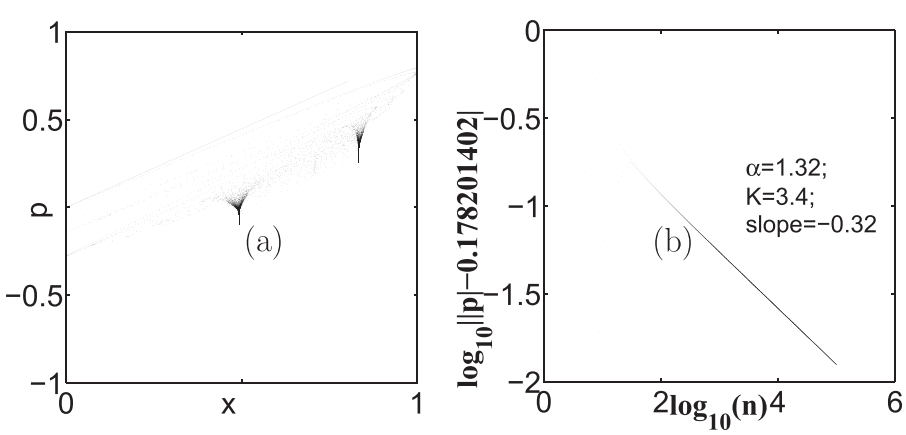

FIG. 6. The Logistic Riemann-Liouville αFM with $\alpha = 1.32$ and $K = 3.4$. (a) Phase space: 300 trajectories with $x_0 = 0$, $p_0 = 10^{-6} + 0.00024i$, $0 \le i < 300$. All converging trajectories converge to the $T = 2$ antisymmetric in p sink. (b) $\log p - \log n$ graph showing the rate of convergence $\delta p \approx n^{-\alpha+1}$ on a single trajectory.

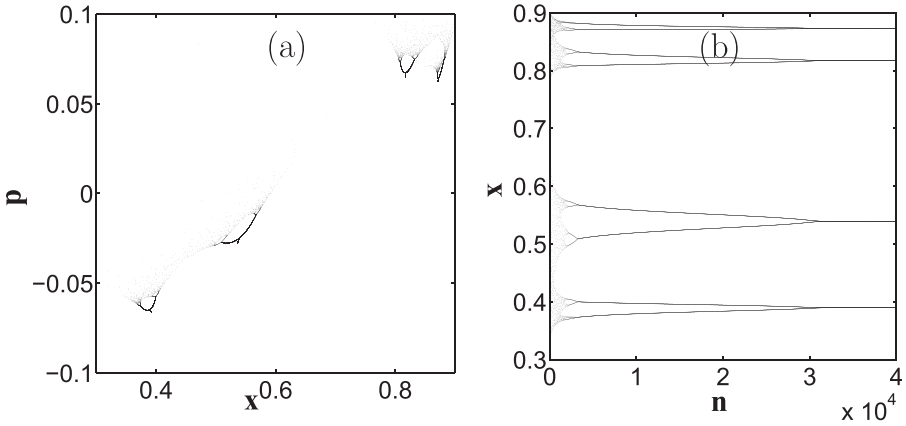

FIG. 7. An inverse CBTT in the Logistic Caputo αFM with $\alpha = 1.2$ and $K = 3.45$. 40 000 iterations on a trajectory with $x_0 = 0.01$ and $p_0 = 0.1$. (a) Phase space. (b) x–n graph.

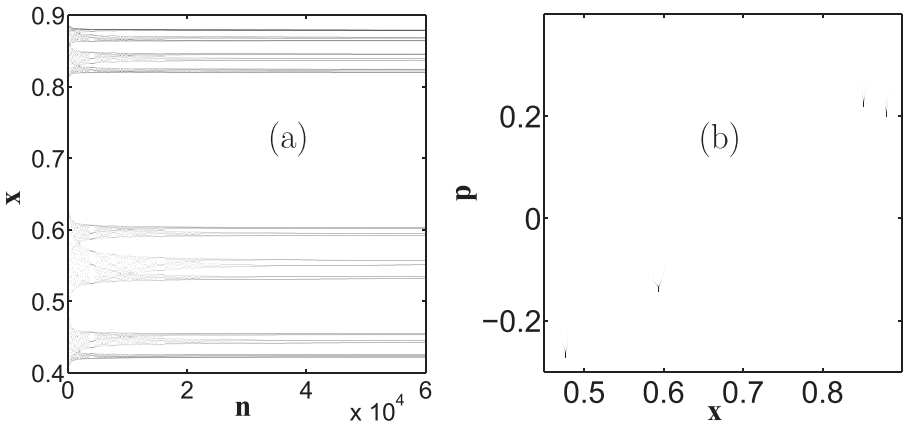

FIG. 8. The Logistic Caputo αFM vs. the Logistic Riemann-Liouville αFM. (a) 60 000 iterations on a single Logistic Caputo αFM trajectory for $\alpha = 1.6$ and $K = 3.9$. (b) The $T = 4$ trajectory for the Logistic Riemann-Liouville αFM with $\alpha = 1.6$ and $K = 3.88$.

$$x_{le}^2 - \left(\frac{2\Gamma(\alpha)}{KV_{\alpha l}} + \frac{K-1}{K}\right)x_{le} + \left(\frac{\Gamma(\alpha)}{2KV_{\alpha l}} + \frac{K-1}{4K}\right)^2 - \frac{(K-1)\Gamma(\alpha)}{K^2V_{\alpha l}} - \frac{(K-1)^2}{2K^2} = 0, \tag{37}$$

which for positive K has solutions only when

$$K \geq K_{c1l} = 1 + \frac{2\Gamma(\alpha)}{V_{\alpha l}}. \tag{38}$$

Direct numeric simulations of the map, Eqs. (29) and (30), confirm this K_{c1l} value as well as the limiting values for p_l, x_{lo}, and x_{le}. For a way to calculate numerically slow converging series Eq. (26) for $V_{\alpha l}$ see Appendix.

In the CBTT band of the Logistic αFM, the narrow band between the upper two curves on Fig. 4(b), the cascade of bifurcation type trajectories exists only in the form of the inverse CBTT (see Fig. 7). The inverse CBTTs that exist for the Logistic Caputo αFM (Figs. 7 and 8(a)) are almost impossible to find in the Logistic Riemann-Liouville αFM (Fig. 8(b)). The closer α is to two, the more difficult it is to find the CBTT in the phase space or x-n graph of the Logistic Caputo αFM.

V. CONCLUSION

The Universal α-Family of Maps introduced in this paper is the extension of the fractional Universal Map, which allows consideration of the Logistic Map as its particular form. The results of the investigation of the Standard and Logistic Families of Maps suggest that the existence of the cascade of bifurcations type trajectories is a general property of the fractional dynamical systems. They appear for the parameter values corresponding to the transition through the period doubling cascade of bifurcations from regular to chaotic motion in the regular dynamics. Figs. 3 and 5 support our statement that with the increase in α, which represents the increase in the systems' dimension and memory (increase in the weights of the earlier states), systems demonstrate more complex and chaotic behavior. Biological systems are systems with memory and the Fractional Logistic Map can serve as a basic model in population biology with memory. We believe that experiments on human memory and/or adaptive biological systems, which in many respects are systems with power law memory, could demonstrate the CBTT-like behavior. New types of materials with memory, such as memristors, memcapacitors, and meminductors, could be used to model fractional systems to demonstrate the existence of the CBTT. The $\alpha > 2$ Standard and Logistic Maps (including their integer volume preserving forms) are topics of ongoing research and their further investigation is necessary to demonstrate the consistency of the changes in the properties of the fractional systems with the change in α.

ACKNOWLEDGMENTS

The author expresses his gratitude to V. E. Tarasov for the useful remarks and to E. Hameiri and H. Weitzner for the opportunity to complete this work at the Courant Institute.

APPENDIX: CALCULATION OF $V_{\alpha l}$

$V_{\alpha l}$ can be written as

$$V_{\alpha l} = \sum_{k=1}^{\infty} (-1)^{k+1} V_\alpha(k) = S_1 + S_2, \tag{A1}$$

where

$$S_1 = \sum_{k=1}^{2N} (-1)^{k+1} V_\alpha(k), \tag{A2}$$

with the N sufficiently large and

$$S_2 = \sum_{k=N+1}^{\infty} \{V_\alpha(2k-1) - V_\alpha(2k)\}. \tag{A3}$$

The value of S_1 can be directly calculated numerically with high precision. The second sum can be developed into a series as follows:

$$\begin{aligned} S_2 &= \sum_{k=N+1}^{\infty} (2k)^{\alpha-3}(\alpha-1)(2-\alpha)\left(1 + \frac{3-\alpha}{2}\frac{1}{k} + \frac{7(3-\alpha)(4-\alpha)}{48}\frac{1}{k^2} + \frac{(3-\alpha)(4-\alpha)(5-\alpha)}{32}\frac{1}{k^3} + O\left(\frac{1}{k^4}\right)\right) \\ &= (2)^{\alpha-3}(\alpha-1)(2-\alpha)\left(\zeta(3-\alpha) + \frac{3-\alpha}{2}\zeta(4-\alpha) + \frac{7(3-\alpha)(4-\alpha)}{48}\zeta(5-\alpha) + \frac{(3-\alpha)(4-\alpha)(5-\alpha)}{32}\zeta(6-\alpha)\right) \\ &\quad - \sum_{k=1}^{N} (2k)^{\alpha-3}(\alpha-1)(2-\alpha)\left(1 + \frac{3-\alpha}{2}\frac{1}{k} + \frac{7(3-\alpha)(4-\alpha)}{48}\frac{1}{k^2} + \frac{(3-\alpha)(4-\alpha)(5-\alpha)}{32}\frac{1}{k^3}\right) + O\left(\frac{1}{N^{6-\alpha}}\right). \end{aligned} \tag{A4}$$

This is what finally was coded using a fast method for calculating values of the ζ-function.

[1] S. G. Samko, A. A. Kilbas, and O. I. Marichev, *Fractional Integrals and Derivatives Theory and Applications* (Gordon and Breach, New York, 1993).
[2] I. Podlubny, *Fractional Differential Equations* (Academic Press, San Diego, 1999).
[3] A. A. Kilbas, H. M. Srivastava, and J. J. Trujillo, *Theory and Application of Fractional Differential Equations* (Elsevier, Amsterdam, 2006).
[4] G. M. Zaslavsky, *Hamiltonian Chaos and Fractional Dynamics* (Oxford University Press, Oxford, 2005).
[5] *Applications of Fractional Calculus in Physics*, edited by R. Hilfer (World Scientific, Singapore, 2000).
[6] *Advances in Fractional Calculus. Theoretical Developments and Applications in Physics and Engineering*, edited by J. Sabatier, O. P. Agraval, and J. A. Tenreiro Machado (Springer, Dordrecht, 2007).
[7] V. E. Tarasov, *Fractional Dynamics: Application of Fractional Calculus to Dynamics of Particles, Fields, and Media* (Springer, HEP, Beijing, 2011).
[8] V. V. Uchaikin, *Fractional Derivatives for Physicists and Engineers* (Springer, HEP, Heidelberg, 2013).
[9] I. Petras, *Fractional-Order Nonlinear Systems* (Springer, HEP, Beijing, 2011).
[10] I. Pan and S. Das, *Intelligent Fractional Order Systems and Control: An Introduction, Studies in Computational Intelligence* (Springer, Heidelberg, 2013).
[11] F. Mainardi, *Fractional Calculus and Waves in Linear Viscoelasticity: An Introduction to Mathematical Models* (Imperial College Press, London, 2010).
[12] V. E. Tarasov, J. Phys.: Condens. Matter **20**, 145212 (2008).
[13] V. E. Tarasov, J. Phys.: Condens. Matter **20**, 175223 (2008).
[14] V. E. Tarasov, Theor. Math. Phys. **158**, 355 (2009).
[15] B. N. Lundstrom, A. L. Fairhall, and M. Maraval, J. Neurosci. **30**, 5071 (2010).
[16] B. N. Lundstrom, M. H. Higgs, W. J. Spain, and A. L. Fairhall, Nat. Neurosci. **11**, 1335 (2008).
[17] J. T. Wixted and E. Ebbesen, Mem. Cognit. **25**, 731 (1997).
[18] A. Toib, V. Lyakhov, and S. Marom, J. Neurosci. **18**, 1893 (1998).
[19] A. L. Fairhall, G. D. Lewen, W. Bialek, and R. R. de Ruyter van Steveninck, Nature **412**, 787 (2001).
[20] D. A. Leopold, Y. Murayama, and N. Logothetis, Cereb. Cortex **13**, 422 (2003).
[21] N. Ulanovsky, L. Las, D. Farkas, and I. Nelken, J. Neurosci. **24**, 10440 (2004).
[22] M. S. A. Zilany, I. C. Bruce, P. C. Nelson, and L. H. Carney, J. Acoust. Soc. Am. **126**, 2390 (2009).
[23] W. Min, G. Luo, B. J. Cherayil, S. C. Kou, and X. S. Xie, Phys. Rev. Lett. **94**, 198302 (2005).
[24] J. T. Wixted, J. Exp. Psychol. Learn. Mem. Cogn. **16**, 927 (1990).
[25] J. T. Wixted and E. Ebbesen, Psychol. Sci. **2**, 409 (1991).
[26] D. C. Rubin and A. E. Wenzel, Psychol. Rev. **103**, 734 (1996).
[27] M. J. Kahana, *Foundations of Human Memory* (Oxford University Press, New York, 2012).
[28] J. R. Anderson, *Learning and Memory: An Integrated Approach* (Wiley, New York, 1995).
[29] A. A. Kilbas, B. Bonilla, and J. J. Trujillo, Dok. Math. **62**, 222 (2000); Demo. Math. **33**, 583 (2000).
[30] V. E. Tarasov, J. Math. Phys. **50**, 122703 (2009); J. Phys. A **42**, 465102 (2009).
[31] A. Wineman, Comput. Math. Appl. **53**, 168 (2007).
[32] A. Wineman, Math. Mech. Solids **14**, 300 (2009).
[33] F. Hoppensteadt, *Mathematical Theories of Populations: Demographics, Genetics, and Epidemics* (SIAM, Philadelphia, 1975).
[34] F. Brauer and C. Castillo-Chavez, *Mathematical Models in Population Biology and Epidemiology* (Springer, New York, 2001).
[35] D. K. Arrowsmith and C. M. Place, *An Introduction to Dynamical System* (Cambridge University Press, Cambridge, 1990); M. Feigenbaum, J. Stat. Phys. **19**, 25 (1978); O. E. Landford, Bull. Am. Math. Soc. **6**, 427 (1982); E. B. Vul, Y. G. Sinai, and K. M. Khanin, Russ. Math. Surv. **39**, 1 (1984); P. Cvitanovic, *Universality in Chaos* (Adam Hilger, Bristol, 1989).
[36] R. Caponetto, G. Dongola, L. Fortuna, and I. Petras, *Fractional Order Systems: Modeling and Control Applications, World Scientific Series on Nonlinear Science Series A* (World Scientific, Singapore, 2010).
[37] L. O. Chua, IEEE Trans. Circuit Theory **18**, 507 (1971).
[38] M. Di Ventra, Y. V. Pershin, and L. O. Chua, Proc. IEEE **97**, 1717 (2009).
[39] J. Trenreiro Machado, Commun. Nonlinear Sci. Numer. Simul. **18**, 264 (2013).
[40] D. Cafagna and G. Grassi, Nonlinear. Dyn. **70**, 1185 (2012).
[41] V. E. Tarasov and G. M. Zaslavsky, J. Phys. A **41**, 435101 (2008).
[42] M. Edelman and V. E. Tarasov, Phys. Lett. A **374**, 279 (2009).
[43] V. E. Tarasov and M. Edelman, Chaos **20**, 023127 (2010).
[44] M. Edelman, Commun. Nonlinear Sci. Numer. Simul. **16**, 4573 (2011).
[45] M. Edelman and L. A. Taieb, *in Advances in Harmonic Analysis and Operator Theory, Operator Theory: Advances and Applications*, edited by A. Almeida, L. Castro, and F.-O. Speck (Springer, Basel, 2013), Vol. 229, pp. 139–155.
[46] M. Edelman, Discontinuity, Nonlinearity, and Complexity **1**, 305 (2012).
[47] N. Heymans and I. Podlubny, Rheol. Acta **45**, 765 (2006).

[48]A. Fulinski, A. S. Kleczkowski, A. Fulinski, and A. S. Kleczkowski, Phys. Scr. **35**, 119 (1987); E. Fick, M. Fick, and G. Hausmann, Phys. Rev. A. **44**, 2469 (1991); K. Hartwich and E. Fick, Phys. Lett. A **177**, 305 (1993); M. Giona, Nonlinearity **4**, 911 (1991); J. A. C. Gallas, Physica A **198**, 339 (1993); A. A. Stanislavsky, Chaos **16**, 043105 (2006).
[49]H. R. Dullin and J. D. Meiss, SIAM J. Appl. Dyn. Syst. **11**, 319 (2012); J. D. Meiss, Commun. Nonlinear Sci. Numer. Simul. **17**, 2108 (2012).
[50]J. Moser, Math. Z. **216**, 417 (1994); H. E. Lomeli and J. D. Meiss, Nonlinearity **11**, 557 (1998).
[51]R. M. May, Nature **261**, 459 (1976).
[52]B. V. Chirikov, Phys. Rep. **52**, 263 (1979); A. J. Lichtenberg and M. A. Lieberman, *Regular and Chaotic Dynamics* (Springer, Berlin, 1992).
[53]M. Hénon, Q. Appl. Math. **XXVII**, 291 (1969).
[54]E. Zeraoulia and J. C. Sprott, *2-D Quadratic Maps and 3-D ODE Systems: A Rigorous Approach* (World Scientific, Singapore, 2010).